# Two-dimensional tungsten oxide nanowire networks

Y. M. Zhao, Y. H. Li, I. Ahmad, D. G. McCartney, Y. Q. Zhu, and W. B. Hu

Citation: Applied Physics Letters **89**, 133116 (2006); doi: 10.1063/1.2357609
View online: http://dx.doi.org/10.1063/1.2357609
View Table of Contents: http://scitation.aip.org/content/aip/journal/apl/89/13?ver=pdfcov
Published by the AIP Publishing

# Two-dimensional tungsten oxide nanowire networks

Y. M. Zhao, Y. H. Li, I. Ahmad, D. G. McCartney, and Y. Q. Zhu[a)]
*School of Mechanical, Materials and Manufacturing Engineering, University of Nottingham, University Park, Nottingham NG7 2RD, United Kingdom*

W. B. Hu
*Hubei Institute for Nationalities, Hubei 445000, China*

(Received 17 May 2006; accepted 9 August 2006; published online 27 September 2006)

The authors report the synthesis and characterization of two-dimensional (2D) single crystalline nanonetworks consisting of tungsten oxide nanowires with diameters of ca. 20 nm. The 2D networks are believed to result from the nanowire growth along the four crystallographic equivalent directions of ⟨110⟩ in the tetragonal $WO_{2.9}$ structure. These 2D tungsten oxide networks may be potential precursors for creating 2D networks comprising $WS_2$ nanotubes. © *2006 American Institute of Physics*. [DOI: 10.1063/1.2357609]

Tungsten oxide nanowire has recently attracted many research interests, being promising in applications such as electrochromic devices, gas sensors, photocatalysts, and electron emitters.[1–5] Another very significant application of tungsten oxide nanowires is its use as a precursor for $WS_2$ nanotube production.[6] Diverse forms of $WO_x$ nanowires have been synthesized in the past few years, and it is found that the resulting compositions ($x$ ranging from 2 to 3), crystal structures (monoclinic, hexagonal, or cubic), and shapes [treelike, three-dimensional (3D) network, or nanobundles] vary dramatically with the preparation techniques. It is well known that the assembly of nanometer-sized building blocks to ordered structures may lead to powerful functions. After the micron-sized treelike monoclinic $W_{18}O_{49}$ structures were obtained,[7] one-dimensional (1D) single crystal nanostructures were produced, e.g., hexagonal $WO_3$ nanowires,[8] monoclinic $W_{18}O_{49}$ nanowires, and $WO_3$ nanosheets.[9] Recently, 3D cubic $WO_3$ nanowire networks have been created.[10] Except for a few hydrothermal syntheses, tungsten oxide nanowires are mostly prepared by the oxidation of metallic W in the form of powders, foils, and filaments. Most recently, we have discovered that inorganic fullerene $WS_2$ nanoparticles can be converted into 1D tungsten oxide nanowires in the presence of water vapor.[11] In this letter, we report the creation of two-dimensional (2D) nanonetworks, consisting of fine tungsten oxide (tetragonal $WO_{2.9}$) nanowires, by a thermal evaporation of commercial $2H$-$WS_2$ particles in a moist atmosphere.

The 2D tungsten oxide nanonetworks were prepared by thermally evaporating a $WS_2$ powder (Aldrich, 99%, particle size less than 2 $\mu$m) under a controlled moist atmosphere. The $WS_2$ powder was placed in the middle of a reaction tube situated in a horizontal tube furnace. Water vapor was introduced into the quartz reaction tube via Ar bubbling [at a flow rate of typically 50 SCCM (SCCM denotes cubic centimeter per minute at STP)] through a wash bottle containing deionized water. Prior to heating the $WS_2$ powder, the reaction tube was flushed with Ar at a flow rate of 200 SCCM for 1 h to remove air residue from the system. Si or quartz substrates were placed at a downstream position of the reaction tube, ca. 20–21 cm away from the $WS_2$ powder where the temperature was around 200–250 °C, for the network collection. After heating for 1 h at 1400–1500 °C, a dark blue deposit formed on the substrate was collected. The as-prepared sample was examined by Siemens D500 x-Ray diffractometer (XRD) and transmission electron microscopy (TEM, JEOL 2000FX, 200 kV). The field emission property was measured in a chamber under a vacuum of less than $2\times10^{-6}$ Torr. A parallel diode structure with an anode-cathode spacing of 250 $\mu$m was used. An indium tin oxide coated glass plate acted as the anode. The threshold field was not measured, since the sample cannot sustain a high current up to 10 mA/cm$^2$.

It is rather difficult to clearly identify the geometry of the as-prepared sample by scanning electron microscopy due to the small size of the 2D networks, but their fluffy ultrafine features are evident. Further investigations by TEM (Fig. 1) have clearly shown that the blue deposit consists of pronounced 2D nanowire networks. The well-defined 2D networks, without a dominant stem in the network construction and similar to the 3D networks,[10] comprise branches with growth directions perpendicular to each other. The nanowires that compose the networks exhibit a uniform diameter of ca. 20 nm, which is about one order of magnitude smaller than those reported in the 3D networks in which nanowires often have a diameter of 200 nm.[10]

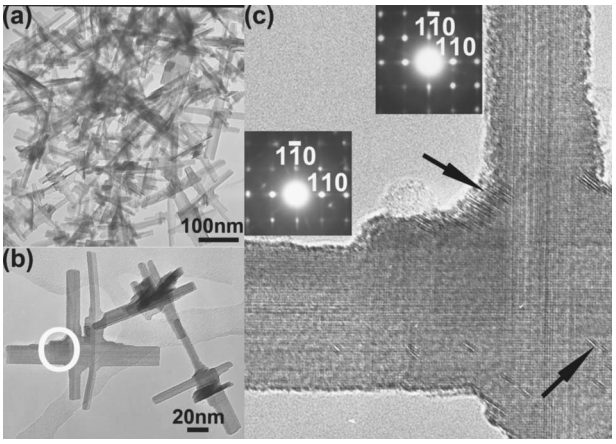


FIG. 1. (a) TEM images of the tungsten oxide nanowire 2D networks and (b) branched 2D networks. (c) High resolution TEM image of the circled area in (b) and the ED patterns of the two branches.

[a)]Author to whom correspondence should be addressed; electronic mail: yanqiu.zhu@nottingham.ac.uk



 

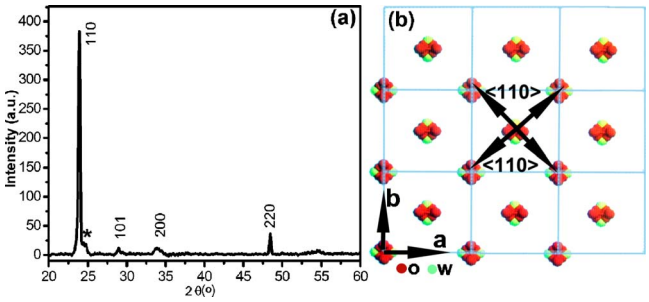


FIG. 2. (Color online) (a) XRD pattern of the tungsten oxide nanowire 2D networks; ( * ) marks a shoulder to the (110) peak. (b) Simulated crystal structure of the tetragonal tungsten oxide in the *a-b* plane.

The XRD pattern of the 2D tungsten oxide networks [Fig. 2(a)] matches well with the tetragonal $WO_{2.9}$ with space group $P4/nmm$ (Ref. 12, $a=b=5.30$ Å and $c=3.83$ Å). A sharp peak appears at 23.8° with the strongest intensity, which is indexed to the (110) plane, and the second strongest peak to the (220) plane. The prominent (110) intensity indicates that the single crystalline nanowires grow along the ⟨110⟩ direction, which has further confirmed by our TEM studies, as shown in Fig. 1(c). A small shoulder to (110) was also observed, indicating the coexistence of a minute amount of other tungsten oxide polytypes with the dominant $WO_{2.9}$, possibly $WO_3$.

A typically four-branched network is shown in Fig. 1(b). The growth directions of any two adjacent branches appear to be perpendicular to each other. A detailed image of the joint and the corresponding electron diffraction (ED) patterns of the two neighboring branches are shown in Fig. 1(c). It appears that both branches grow along ⟨110⟩, consistent with the XRD results. The plane separation of 3.7 nm also agrees well with the interplanar spacing of {110}. It has proven to be difficult to obtain a distinct ED pattern of the joint due to its small area (only 20 nm wide) and the spot size limitation of the electron beam. A whole 2D network appears to be a single crystal, because the lattice fringes representing the crystal planes are continuously throughout the entire junction area and no grain boundaries have been observed, as shown in Fig. 1(c). The arrowed areas in Fig. 1(c) show some planar crystalline defects at the corner or in the middle of the network. It is noteworthy that for some networks, e.g., the other two shown in the right of Fig. 1(b), the crystal structures in the joint areas are not easy to observe directly as illustrated in Fig. 1(c), because short tungsten oxide nanowires or particles are stuck or stacked above each other and cover the junction areas.

A question arises as to how the 2D tungsten oxide network is formed. Apparently, there is no catalyst involved during the synthesis, and furthermore no liquid droplet feature occurred at the nanowire tip; thus the well-known vapor-liquid-solid mechanism cannot account for this growth.[13–15] It is understood that in many cases intrinsic structural defects, such as twin defects, planar defects, or stacking faults, will contribute to the nanowire growth as they form preferential steps for incoming atoms to deposit.[16–18] The vapor to solid transformation mediated by defective sites may be able to explain the nanowire growth. In Fig. 1(c), the streaks that occurred in the ED patterns of the nanowires are indicative of planar oxygen vacancies within the {110} planes, which is similar to that found in computer simulation of the tungsten oxide nanowires.[19] The 2D networks seem most likely to

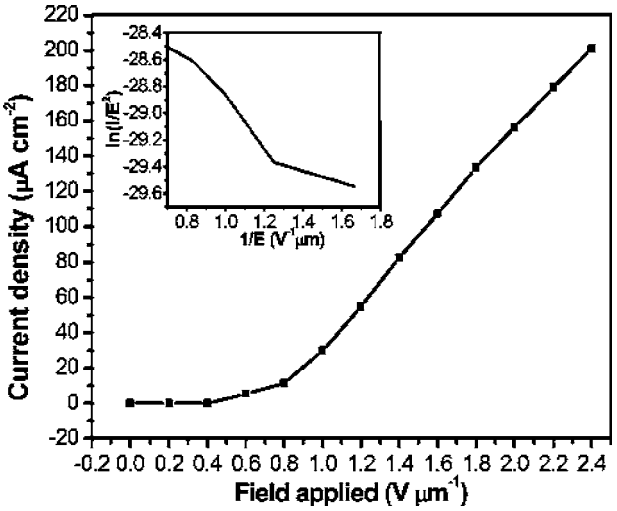


FIG. 3. Field emission properties of the 2D tungsten oxide networks and its corresponding FN plot (inset).

form due to the four crystallographically equivalent [110] directions in the *a-b* planes of the tetragonal $WO_{2.9}$. This is different from the reported 3D tungsten oxide networks in which the crystal structure of the nanowires is cubic $WO_3$ with six equivalent growth directions along ⟨100⟩. It is suggested that the crystalline symmetry of the resulting tungsten oxide nanowires is the key reason for the growth of either a 2D network or a 3D network. Figure 2(b) shows a simulation by CERIUS2 of the tetragonal $WO_3$ crystal structure in the *a-b* plane, by adopting parameters such as $a=b=5.272$ Å, $c=3.920$ Å, and space group $P4/nmm$ from the ICSD database. The oxygen positions in the *a-b* plane of the nonstoichiometric tetragonal $WO_{2.9}$ may shift slightly compared with the unreduced tetragonal $WO_3$ while this is the closest match available to the lattice constant.[19] Figure 2(b) suggests that the tungsten and oxygen atoms are close packed in {110} planes; therefore the nanowires grow preferentially along the four equivalent ⟨110⟩ directions, leading to 2D networks. As a consequence, the intensity of the (110) peak in the XRD pattern exhibits a dominant characteristic.

To prepare the sample for the field emission measurement, a Si substrate was placed at the downstream position in the reaction tube where the 2D nanonetworks form. The field emission current versus electric field for the as-prepared 2D nanonetworks on Si was measured at a vacuum gap of 250 $\mu$m, as shown in Fig. 3. The Fowler-Nordheim (FN) fit (inset) does not exhibit a perfectly straight line but it generally reflects that the electron emission from the tips of the nanowires follows the FN behavior. If the turn-on field ($E_{to}$) is defined as the macroscopic field required to produce a current density of 10 $\mu A/cm^2$, we then obtain a turn-on field of 0.74 V/$\mu$m for the 2D networks, as shown in Fig. 3. This value is apparently much lower than many of those observed for other tungsten oxide nanowires;[5,10,20,21] however, many factors may affect the turn-on field, such, as the chemical composition, size, shape, and even the sample preparation techniques. Nevertheless, the ultrasmall diameter of 20 nm of the nanowires and the unique 2D network structures may have both contributed to the low turn-on field, making them good candidates for future field emission nanodevices.

Our preliminary results have also shown that such 2D tungsten oxide networks can be converted to 2D nanotube networks made of $WS_2$. Figure 4 shows a typical TEM im-

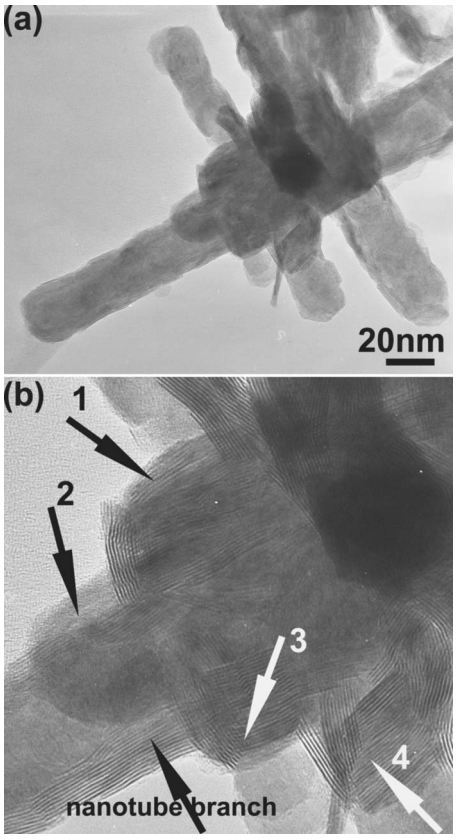


FIG. 4. TEM images of 2D $WS_2$ nanotube networks. (a) A single 2D network; (b) enlargement of the central area in (a). Arrows 1, 2, 3, and 4 refer to small nanotubes present at the junction area.

age of a 2D nanotube network obtained by directly reacting 2D tungsten oxide networks with $H_2S$ (at a flow rate of 30 SCCM) at 850 °C for 30 min. Figure 4(a) shows that the $WS_2$ nanotubes inherited the original geometry of the 2D oxide networks, although many structural defects are observed. Rothschild *et al.* have established a mechanism for the growth of $WS_2$ nanotubes from tungsten oxide particles or whiskers under a gas mixture of $H_2$, $N_2$, and $H_2S$.[6] In that model, an oxide whisker first reacts with $H_2S$ to form a $WS_2$ monomolecular skin, and the inner oxide core to $WS_2$ conversion was then controlled by a slow diffusion. The hydrogen plays a reducing role and promotes 1D elongation of the $WO_{3-x}$ $(x<1)$ nanorods. During the oxide core reduction, the formation of crystallography shear planes due to the oxygen vacancies will rearrange until reaching a stable reduced oxide phase, such as $W_{18}O_{49}$. The highly ordered nature of the reduced oxide provides a kind of template for the sulfide layer growth. A similar mechanism should be applicable to current 2D $WS_2$ nanotubes formation. As discussed above in the $WO_{2.9}$ nanonetwork formation, planar defects of oxygen vacancies may exist along the growth direction of the nanowires, which will facilitate the sulfide layer growth. Although there was no $H_2$ involved in our reaction, $WS_2$ nanotube structures were obtained without a substantial morphological change.

It is noted that small nanotubes [numbered 1, 2, 3, and 4 in Fig. 4(b)] are often present in the junction area, alongside with the expected nanotube branches originating from the initial oxide branches. The complex junctions in the nanotube networks may be associated with the original defective junctions within the oxide networks, as shown in the right of Fig. 1(b). These defective sites are likely to coalesce with adjacent small tungsten oxide particles owing to the high surface activity,[22] eventually leading to irregular nanotubes in the joint areas. Improvement of the structure of the 2D nanotube networks is currently under investigation. It is believed that high quality 2D tungsten disulfide nanotube networks, which may exhibit excellent properties that simple 1D nanotubes do not possess, will be of great importance for nanoscience and nanotechnology.

In summary, we have generated 2D tungsten oxide nanowire networks using a thermal evaporation of $WS_2$ powder in the presence of water vapor. The nanowires that compose the 2D networks are highly uniform, with a diameter of ca. 20 nm. XRD and TEM studies indicated that the oxide networks are tetragonal $WO_{2.9}$. The nanowires are believed to grow along the four crystallographic equivalent growth directions of $\langle 110 \rangle$, leading to the formation of a 2D network.

The 2D tungsten oxide networks can be employed as precursors for the creation of 2D tungsten disulfide nanotube networks.

The authors thank the EPSRC (UK) for financial support. The authors would like to thank the use of the EPSRC's Chemical Database Services at Daresbury. Thanks are also due to Q. Zhang, J. Q. Li, and Z. F. Shi of NTU (Singapore) for the field emission measurements.

[1] J. G. Liu, Z. J. Zhang, Y. Zhao, X. Su, S. Liu, and E. Wang, Small **1**, 310 (2005).
[2] C. Sanrato, M. Odziemkowski, M. Ulmann, and J. Augustynski, J. Am. Chem. Soc. **123**, 10639 (2001).
[3] S. H. Baeck, K. S. Choi, T. F. Jaramillo, G. D. Stucky, and E. W. McFarland, Adv. Mater. (Weinheim, Ger.) **15**, 1269 (2003).
[4] W. M. Qu and W. Wlodarski, Sens. Actuators B **64**, 42 (2000).
[5] Y. B. Li, Y. S. Bando, and D. Golberg, Adv. Mater. (Weinheim, Ger.) **15**, 1294 (2003).
[6] A. Rothschild, J. Sloan, and R. Tenne, J. Am. Chem. Soc. **122**, 5169 (2000).
[7] Y. Q. Zhu, W. B. Hu, W. K. Hsu, M. Terrones, N. Grobert, J. P. Hare, H. W. Kroto, D. R. M. Walton, and Humberto Terrones, Chem. Phys. Lett. **309**, 327 (1999).
[8] Z. J. Gu, Y. Ma, W. S. Yang, G. J. Zhang, and J. N. Yao, Chem. Commun. (Cambridge) **2005**, 3597.
[9] H. G. Choi, Y. H. Jung, and D. K. Kim, J. Am. Ceram. Soc. **88**, 1684 (2005).
[10] J. Zhou, Y. Ding, S. Z. Deng, L. Gong, N. S. Xu, and Z. L. Wang, Adv. Mater. (Weinheim, Ger.) **17**, 2107 (2005).
[11] Y. H. Li, Y. M. Zhao, R. Z. Ma, Y. Q. Zhu, and N. Fisher J. Phys. Chem. B **110**, 18191 (2006).
[12] JCPDS-International Center for Diffraction Data, Card No. 00-018-1417 (unpublished).
[13] R. S. Wagner and W. C. Ellis, Appl. Phys. Lett. **4**, 89 (1964).
[14] Y. Y. Wu and P. D. Yang, J. Am. Chem. Soc. **123**, 3165 (2001).
[15] P. X. Gao and Z. L. Wang, J. Phys. Chem. B **108**, 7534 (2004).
[16] G. W. Zhou, Z. Zhang, Z. G. Bai, S. Q. Feng, and D. P. Yu, Appl. Phys. Lett. **73**, 677 (1998).
[17] H. Z. Zhang, Y. C. Kong, Y. Z. Wang, X. Du, Z. G. Bai, J. J. Wang, D. P. Yu, Y. Ding, Q. L. Hang, and S. Q. Feng, Solid State Commun. **109**, 677 (1999).
[18] X. Liu, X. H. Wu, H. Cao, and R. P. H. Chang, J. Appl. Phys. **95**, 3141 (2004).
[19] A. Aird, M. C. Domeneghetti, F. Mazzi, V. Tazzoli, and E. K. H. Salje, J. Phys.: Condens. Matter **10**, L569 (1998).
[20] J. G. Liu, Z. J. Zhang, Y. Zhao, X. Su, S. Liu, and E. G. Wang, Small **1**, 310 (2005).
[21] J. Zhou, L. Gong, S. Z. Deng, J. Chen, J. C. She, N. S. Xu, R. S. Yang, and Z. L. Wang, Appl. Phys. Lett. **87**, 223108 (2005).
[22] H. A. Therese, J. X. Li, U. Kolb, and W. Tremel, Solid State Sci. **7**, 67 (2005).